Max-Planck-Institut
für Mathematik
in den Naturwissenschaften
Leipzig

Stable focal inverse source localization using combinatorial optimization techniques combined with regularization methods

by

C. H. Wolters, R. Beckmann, A. Rienäcker and H. Buchner

Preprint-Nr.: 59 1998

Stable Focal Inverse Source Localization using Combinatorial Optimization Techniques combined with Regularization Methods

running title: Stable Focal Inverse Source Localization

C. H. Wolters, MSc[1], R. Beckmann,MEng[2], A. Rienäcker, PhD[3] and Prof. H. Buchner,MD[2]

(1) Max-Planck-Institute of Cognitive Neuroscience and Max-Planck-Institute for Mathematics in the Sciences, Leipzig, Germany
(2) Department of Neurology, RWTH Aachen, Germany
(3) Institute for Machine Elements and Tribology, University of Kassel, Germany

Abstract

The inverse problem arising from EEG and MEG is largely underdetermined. One strategy to alleviate this problem is the restriction to a limited number of point-like sources, the *focal source model*. Although the singular value decomposition of the spatio-temporal data gives an estimate of the minimal number of dipoles contributing to the measurement, the exact number is unknown in advance and noise complicates the reconstruction. Classical nonlinear dipole fit algorithms do not give an estimate for the correct number because they are not stable with regard to an overestimation of this parameter. Too many sources may only describe noise, but can still attain a large magnitude during the inverse procedure and may be indiscernible from the true sources. This paper describes a nonlinear dipole fit reconstruction algorithm with a new regularization approach for the embedded linear problem, automatically controlled by the noise in the data and the condition of the occuring least square problems. The algorithm is stable with regard to source components which "nearly" lie in the kernel of the projection or lead field operator and it thus gives an estimate of the unknown number parameter. Simulation studies in a simulated sulcus structure are carried out for an instantaneous dipole model and spatial resolution in the sulcus and stability of the new method are compared with a classical reconstruction algorithm without regularization.
keywords: EEG; dipole fit; simulated annealing; regularization; truncated singular value decomposition; finite element method

Introduction

Source localization of cerebral activity with respect to the individual anatomy is a prominent goal of electro- and magnetoencephalography. The determination of the current distribution inside the brain by means of extracranial field measurements is called the inverse problem. The non-uniqueness of the inverse problem implies that assumptions on the source model, as well as anatomical and physiological a-priori knowledge about the source region and sometimes even results from other techniques like functional magnetic resonance imaging ([Menon *et al.*, 1997],[Opitz *et al.*, to appear]) should be taken into account to obtain a unique solution.

Different source models have been developed during the last years. One possibility is the restriction to a limited number of dipoles, the *focal source model* ([Scherg and von Cramon, 1985],[Vaughan, 1974]). The various spatio-temporal focal source models differ in the manner in which they describe the time dependence of the data. Generally, they are grouped into three classes, the unconstrained dipole model (so-called *moving dipole*), dipoles with temporally fixed location (*rotating dipole*) and dipoles with fixed location and fixed orientation (*fixed dipole*). If only one single time "snapshot" is taken into account, the three classes merge in a spatial dipole model, the so-called *instantaneous state dipole model* [Wood, 1982].

Another possibility is the *distributed source model*, where the restriction to a limited number of focal sources is abolished. The non-uniqueness of the resulting problem is compensated by the assumption that the dipole distribution should be minimal with regard to a specific norm. Different norms have been proposed, such as the linear L2-norm [Hämäläinen and Ilmoniemi, 1994], leading to a smooth current

distribution with minimal source energy and the nonlinear L1-norm ([Rienäcker *et al.*, 1997],[Wagner *et al.*, 1994]), which results in a more focal distribution.
This paper deals with the focal source model. [Mosher *et al.*, 1992] showed how a common linear algebraic framework can be formulated for the three spatio-temporal dipole models. One can conclude from this formulation that measured fields depend nonlinearly on dipole location and fixed orientation and linearly on dipole moment strength. Thus, after having chosen the number of sources, nonlinear algorithms should determine their locations (and possibly fixed orientations) and embedded linear methods their moment strength. Another important parameter is the number of active source components, which is normally unknown in advance, but which is required as an input parameter for spatio-temporal dipole modeling. One possibility for the determination of the number parameter was described by [Mosher *et al.*, 1992]. They proposed to separate the signal and noise subspaces and thus to visually determine the number of source components through the drop in the magnitude of the smallest signal eigenvalue to the greatest noise eigenvalue of the estimated data covariance matrix $\frac{1}{(n-1)}\mathbf{F}\mathbf{F}^{tr}$ (n: number of samples, m: number of channels, $n \times m$ matrix $\mathbf{F}$: measured data). This procedure assumes that the signals have a sufficient strength and that they are sufficiently uncorrelated during the time interval. An algorithmic way for the determination of the number parameter is offered by information criteria [Knösche *et al.*, to appear]. Under the assumption that the measurements are noise-free and the rank of the projection or lead field operator is maximal (i.e. no source component projects in the data null space), the number of non-zero eigenvalues of the data covariance matrix equals the number of independent source components. Information criteria are based on a statistical concept of separating the space spanned by the principal components of the estimated data covariance matrix into a signal and a noise part.
We will present a "trial and error" strategy to combine the determination of the unknown number parameter with the localization of the sources using a nonlinear dipole fit method with a new regularization approach. The nonlinear dipole parameters will be calculated iteratively by means of combinatorial optimization techniques such as simulated annealing (SA) which globally minimizes a cost function ([Buchner *et al.*, 1997],[Gerson *et al.*, 1994],[Haneishi *et al.*, 1994]). The linear parameters will then be determined by linear least square methods, yielding a "best" (will be defined) fit between measured and calculated electric potentials and magnetic inductions. If dipole components are proposed which "numerically" (nearly) project into the data null space, the corresponding lead field matrix becomes ill-conditioned. In combination with noisy data, simple least square algorithms based on singular value or QR-decompositions like the complete orthogonal factorization method (COF) can yield physiologically unexplainable results for dipole moment strengths, especially when overestimating the number of active sources. This problem can be solved with so called regularization methods like the truncated singular value decomposition (TSVD)[Wolters *et al.*, 1997] or Tikhonov-Phillips regularization [Fuchs *et al.*, 1998]. After presenting the theory with regard to the different spatio-temporal dipole models, simulation studies using the instantaneous state dipole model will be carried out to show, that the SA-TSVD is able to reconstruct a reference configuration in the case of noisy EEG-data, even when overestimating the number of active

sources and is thus be able to give an estimate of the unknown number parameter.

A physiological a-priori information about the source region (*influence space*) is the assumption that the generators must be located on the folded surface of the brain inside the cortex, ignoring white matter and deeper structures such as basal ganglia, brain stem and cerebellum. Another addition is the anatomical information that the apical dendrites of the large pyramid cells in the cortex which are considered the generators of the measured fields are perpendicular to the surface of the cortex ([Lorente de No, 1938],[Nunez, 1990]). This limitation to normally oriented dipoles is called the *normal-constraint*. Because a mathematical dipole models an active source region with a certain extent and the resolution of the inverse current reconstruction is limited, the influence space can be discretized. In our simulations with the program CAUCHY [Buchner *et al.*, 1997], we used a "cortical" surface mesh (discrete influence space) and dipoles could only be placed on the mesh nodes (*influence nodes*). If the discretization of the surface is fine enough to capture geometric details, the normal-constraint will be a suitable model.
The inverse algorithm strongly depends on the quality of a forward method. Here, the potential and magnetic field distribution of the observation space is calculated for a known source. Essential for the accuracy is an appropriate model of the volume conductor and of the field propagation. Since the temporal derivatives of the field measures are negligible for typical EEG/MEG frequencies [Plonsey and Heppner, 1967], their propagation can be described by the quasistatic approximation of Maxwells system of coupled partial differential equations (PDE), leading to a second order elliptic PDE to be solved for the potential. It can be shown, that the solution of this equation in the variational formulation in combination with boundary conditions of Neumann-type and a Dirichlet-point (reference electrode) exists and is unique [Wolters, 1997]. Thus, the finite element method can be applied to numerically calculate the potential distribution inside the volume conductor ([Bertrand *et al.*, 1991], [van den Broek *et al.*, 1996], [Buchner *et al.*, 1997]). This method allows anisotropic and inhomogeneous conductivities ([Haueisen *et al.*, 1995], [Marin *et al.*, 1998],[Pohlmeier *et al.*, 1997]).
Since the differential equation is linear, it is possible to set up a so-called influence or *lead field matrix* $\mathbf{L}$. A column of $\mathbf{L}$ is established by calculating a forward solution at the measurement nodes for a dipole on an influence node with unit strength in one direction. If the physiological a-priori information and the normal-constraint are applied, there is only one possible dipole direction for each influence node and thus every dipole location is represented by only one column in the lead field matrix and one row in the strength matrix. For the unconstrained case, three columns in $\mathbf{L}$ represent the three orthogonal unit dipoles at a specific location and three rows in the strength matrix $\mathbf{J}$ correspond to their time series. For an arbitrary dipole source configuration $\mathbf{J}$, the resulting electric potentials and magnetic inductions can then be inexpensively calculated by

$$\mathbf{\Phi}^c = \mathbf{L}\mathbf{J}.$$

An important point is the localization of active neuron assemblies within deep and narrow fissures and sulci because two-thirds of the cerebral cortex lie within these structures and MEG is most sensitive to them. An especially difficult case is the

reconstruction of oppositely oriented sources if both sulcus walls have regions of neuronal activity.
In the next section, we will present the underlying theory of the focal inverse current reconstruction algorithms SA-COF and SA-TSVD and we will compare the regularization concept of the TSVD with Tikhonov-Phillips regularization. SA-COF and SA-TSVD have been implemented in CAUCHY and EEG simulation studies using the instantaneous state dipole model have been carried out in a four-sphere model with a simulated sulcus structure embedded in the innermost sphere. The goal was the examination of the localization properties, i.e. spatial resolution and stability, of both algorithms in the sulcus.

Theory

The goal of the focal inverse current reconstruction is to find a location tupel q for a chosen number of p dipoles of the influence space and the corresponding $r \times n$ strength matrix $\mathbf{J}$ such that

$$H(q) = ||\mathbf{L_q J} - \mathbf{\Phi}^m||_F^2 \stackrel{!}{=} \min$$

where the $m \times r$ matrix $\mathbf{L_q}$ is the overdetermined lead field matrix (thus $m > r$), corresponding to the location tupel q, the $m \times n$ matrix $\mathbf{\Phi}^m$ are the noise-free measurements (EEG/MEG), where m is the number of channels and n the number of samples and $||\cdot||_F$ is the Frobenius-norm. Using the normal-contraint, the number r of columns of $\mathbf{L_q}$ and rows of $\mathbf{J}$ equals the number p of dipoles, without this constraint it is $r = 3p$.
The minimization task can be split into two problems. First, a physiologically and mathematically suitable model should be developed for the shape of the functional graph H. Every evaluation of H for a given location tupel q contains the construction of the corresponding lead field matrix $\mathbf{L_q}$ and the subsequent determination of the direction and strength matrix $\mathbf{J}$ with respect to the noise in the measured data $\mathbf{\Phi}_\epsilon^m$. The second problem is to find the dipole location tupel q which gives a good approximation of the global minimum of H in a feasible calculation time. This was realized with the SA-algorithm implemented in CAUCHY.
We will start with the derivation of the theory for a single timepoint $n = 1$ since the instantaneous state dipole model was used for the sulcus simulations. Notationally, we use underlines to indicate vectors and boldface for matrices. The measured and noisy data vector will be denoted as $\underline{\Phi}_\epsilon^m$, the noise as $\underline{\Delta\Phi}^m$ and the noiseless data as $\underline{\Phi}^m = \underline{\Phi}_\epsilon^m - \underline{\Delta\Phi}^m$ and our problem reduces to

$$H(q) = ||\mathbf{L_q}\underline{J} - \underline{\Phi}^m||_2^2 \stackrel{!}{=} \min. \tag{1}$$

Assuming that a dipole location tupel q has been proposed by the SA-algorithm, the linear least square problem (1) with noisy data $\underline{\Phi}_\epsilon^m$ should then be solved. One solution strategy is based on the well-known singular value decomposition (SVD)

$$\mathbf{L}_q = \mathbf{USV}^{tr} = (\underline{u}_1, \ldots, \underline{u}_m) \begin{pmatrix} \mathbf{\Sigma} \\ \mathbf{0} \end{pmatrix} (\underline{v}_1, \ldots, \underline{v}_r)^{tr}$$

with the orthogonal $m \times m$ matrix $\mathbf{U}$, the $m \times r$ matrix $\mathbf{S}$ with $\mathbf{\Sigma} = diag(\varsigma_1, \ldots \varsigma_r)$ and the orthogonal $r \times r$ matrix $\mathbf{V}$. ς_i are called the *singular values* of $\mathbf{L}_q$ and they are automatically arranged by the SVD such that $\varsigma_1 \geq \varsigma_2 \geq \ldots \geq \varsigma_r > 0$, if we assume that $\mathbf{L}_q$ has full column rank. $\underline{v}_i$ are the so-called *right singular vectors* and $\underline{u}_i$ the *left singular vectors*, both arranged with increasing spatial frequency. It can be shown, that ς_i^2 are the eigenvalues and $\underline{u}_i$ the eigenvectors of $\mathbf{L}_q \mathbf{L}_q^{tr}$ and ς_i^2 the eigenvalues and $\underline{v}_i$ the eigenvectors of $\mathbf{L}_q^{tr} \mathbf{L}_q$. Furthermore, it is

$$\mathbf{L}_q \underline{v}_i = \varsigma_i \underline{u}_i \qquad i = 1, \ldots, r, \tag{2}$$

and

$$\begin{aligned} \underline{u}_i^{tr} \mathbf{L}_q &= \varsigma_i \underline{v}_i^{tr}, \qquad i = 1, \ldots, r, \\ \underline{u}_i^{tr} \mathbf{L}_q &= \underline{0}^{tr}, \qquad i = r+1, \ldots, m. \end{aligned} \tag{3}$$

Thus, the space spanned by $\{\underline{u}_1, \ldots, \underline{u}_r\}$ is called the *column space* and $span\{\underline{u}_{r+1}, \ldots, \underline{u}_m\}$ is the so-called *left null space* of $\mathbf{L}_q$. Let $\mathbf{U}_r$ be the $m \times r$ matrix $\mathbf{U}_r = (\underline{u}_1, \ldots, \underline{u}_r)$. Without respect to the noise in the data, (1) can be solved by means of the generalized inverse of the lead field matrix [Miller, 1979]

$$\underline{J}^+ = \mathbf{L}_q^+ \underline{\Phi}_\epsilon^m = \sum_{i=1}^{r} \frac{1}{\varsigma_i} < \underline{\Phi}^m + \underline{\Delta\Phi}^m, \underline{u}_i > \underline{v}_i, \tag{4}$$

($< \cdot, \cdot >$ denotes the vector scalar product), in matrix form

$$\begin{aligned} \mathbf{L}_q^+ \underline{\Phi}_\epsilon^m &= \left(\mathbf{L}_q^{tr} \mathbf{L}_q\right)^{-1} \mathbf{L}_q^{tr} \underline{\Phi}_\epsilon^m = \mathbf{V} \mathbf{S}^+ \mathbf{U}^{tr} \underline{\Phi}_\epsilon^m \\ &= (\underline{v}_1, \ldots, \underline{v}_r) \begin{pmatrix} \mathbf{\Sigma}^{-1} & \mathbf{0} \end{pmatrix} (\underline{u}_1, \ldots, \underline{u}_m)^{tr} \underline{\Phi}_\epsilon^m. \end{aligned}$$

Usual nonlinear dipole fit methods use this generalized inverse to solve the linear least square problems embedded in the nonlinear optimization process.
The matrix $\mathbf{P}_L = \mathbf{L}_q \mathbf{L}_q^+$ projects data $\underline{\Phi}$ onto the column space of $\mathbf{L}_q$

$$\mathbf{P}_L \underline{\Phi} = \mathbf{L}_q \mathbf{L}_q^+ \underline{\Phi} \overset{(4)}{=} \mathbf{L}_q \sum_{i=1}^{r} \frac{1}{\varsigma_i} < \underline{\Phi}, \underline{u}_i > \underline{v}_i \overset{(2)}{=} \sum_{i=1}^{r} < \underline{\Phi}, \underline{u}_i > \underline{u}_i = \mathbf{U}_r \mathbf{U}_r^{tr} \underline{\Phi}.$$

[Mosher *et al.*, 1992] derived an efficient form of calculating $H(q)$, which is based on a SVD of the data matrix $\mathbf{\Phi}_\epsilon^m = \mathbf{U}_\Phi \mathbf{S}_\Phi \mathbf{V}_\Phi^{tr}$:

$$\begin{aligned} H(q) &= ||\mathbf{\Phi}_\epsilon^m - \mathbf{L}_q \mathbf{J}^+||_F^2 = ||\mathbf{\Phi}_\epsilon^m - \mathbf{L}_q (\mathbf{L}_q^+ \mathbf{\Phi}_\epsilon^m)||_F^2 = ||\mathbf{\Phi}_\epsilon^m||_F^2 - ||\mathbf{P}_L \mathbf{\Phi}_\epsilon^m||_F^2 \\ &= ||\mathbf{U}_\Phi \mathbf{S}_\Phi \mathbf{V}_\Phi^{tr}||_F^2 - ||\mathbf{U}_r \mathbf{U}_r^{tr} \mathbf{U}_\Phi \mathbf{S}_\Phi \mathbf{V}_\Phi^{tr}||_F^2 = ||\mathbf{S}_\Phi||_F^2 - ||\mathbf{U}_r^{tr} \mathbf{U}_\Phi \mathbf{S}_\Phi||_F^2 \end{aligned}$$

Orthogonal matrices were dropped in the derivation since they preserve the Frobenius-norm. When using SVD-versions of the lead field matrix, in which only the left singular vectors $\mathbf{U}_r$ are iteratively calculated and when r is small relative to m, this procedure of calculating $H(q)$ will outperform methods based on noniterative QR-decompositions, leading to the same result. Nevertheless, in our simulations we used a Complete Orthogonal Factorization of the lead field matrix (COF), based on

a QR-decomposition and included in the LAPACK-library (Linear Algebra PACKage). The SA-COF will represent the focal current reconstruction methods without regularization.
In practice, $\mathbf{L_q}$ is often ill-posed during the SA-optimization process. This can be measured with the condition number of the lead field matrix $cond_2(\mathbf{L_q}) = \frac{\varsigma_1}{\varsigma_r}$, which can be quite large. Thus, the singular values, ς_i, get very small and the high spatial frequency components of the noise in the data can be extremely amplified (see equation (4)). This has an effect on those spatial dipole components, which "numerically" (nearly) lie in the kernel of $\mathbf{L}_q$. It can lead to source configurations, where dipoles with a large strength nearly cancel each other with regard to their surface potential distribution, and only explain noise or where radial dipoles get a big strength only to explain MEG noise, especially if the number of active sources is overestimated. The problem can be solved with a regularization of the generalized inverse

$$\underline{J}_\gamma = T_\gamma \underline{\Phi}_\epsilon^m = \sum_{i=1}^{r} \frac{1}{\varsigma_i} F_\gamma(\varsigma_i) < \underline{\Phi}_\epsilon^m, \underline{u}_i > \underline{v}_i,$$

where F_γ is called a filter [Louis, 1989]. The choice of

$$F_\gamma(\varsigma) = \frac{\varsigma^2}{\varsigma^2 + \gamma^2}$$

leads to a Tikhonov-Phillips regularization, where the high spatial frequency components in the source space, strongly influenced by the noise in the data space, are attenuated and the condition number of the regularized linear least square problem

$$||\bar{\mathbf{L}}_q \underline{J} - \bar{\Phi}_\epsilon^m||_2^2 \stackrel{!}{=} \min$$

with

$$\bar{\mathbf{L}}_q = \begin{pmatrix} \mathbf{L_q} \\ \gamma I \end{pmatrix}$$

and

$$\bar{\Phi}_\epsilon^m = \begin{pmatrix} \underline{\Phi}_\epsilon^m \\ 0 \end{pmatrix}$$

is ameliorated to $cond_2(\bar{\mathbf{L}}_q) = \sqrt{\frac{\varsigma_1^2+\gamma^2}{\varsigma_r^2+\gamma^2}}$ [Hämmerlin and Hoffmann, 1991]. This regularization concept for nonlinear dipole fit methods has recently been applied to source localization [Fuchs *et al.*, 1998].

Another way is to choose the filter

$$F_\gamma(\varsigma) = \begin{cases} 1, \text{ if } \varsigma \geq \gamma \\ 0, \text{ if } \varsigma < \gamma \end{cases},$$

leading to a regularization called the *Truncated Singular Value Decomposition* (TSVD). This algorithm is simply to implement and has the effect of a lowpass filter. The high spatial frequency components of the data, $\varsigma_i < \underline{J}, \underline{v}_i > \underline{u}_i$, are lying below the noise level and as a consequence, the high spatial frequency components in the

source space cannot be reconstructed. Using regularization, information will be lost but otherwise the amplification of the high frequency data components would have a more negative effect on the solution, especially in combination with an overestimation of the number of active sources. Like Tikhonov-Phillips regularization, the TSVD ameliorates the condition of the problem.

The proposed algorithm is an iterative procedure. In every step of the optimization, $\mathbf{L_q}$ is changing and thus the condition of the least square problem. Therefore, an automatic determination of the regularization parameter γ is essential. One possibility is provided by the discrepancy principle ([Vainikko, 1982],[Vainikko, 1983]) where the so-called *defect* d to the measured data

$$\begin{aligned} d = ||(I - \mathbf{L_q} T_\gamma)\underline{\Phi}_\epsilon^m||_2^2 &= ||\underline{\Phi}_\epsilon^m - \sum_{i=1}^{r} F_\gamma(\varsigma_i) < \underline{\Phi}_\epsilon^m, \mathbf{u}_i > \mathbf{u}_i||_2^2 \\ &= ||\underline{\Phi}_\epsilon^m||_2^2 - \sum_{i=1}^{r} F_\gamma(\varsigma_i) | < \underline{\Phi}_\epsilon^m, \mathbf{u}_i > |^2 \\ &= ||\underline{\Phi}_\epsilon^m||_2^2 - \sum_{\varsigma_i > \gamma} | < \underline{\Phi}_\epsilon^m, \mathbf{u}_i > |^2 \end{aligned}$$

is not only minimized, but chosen in dependence of the condition number of $\mathbf{L_q}$ and of the noise $\underline{\Delta\Phi}^m$ in the data.
Let $\mathbf{C}_N$ be the $m \times m$ sample noise covariance matrix, determined e.g. from the signal-free pre-stimulus interval of the measurements, averaged over all epochs. This matrix reflects the spatial distribution and correlation of the noise. $\mathbf{C}_N$ is a symmetric and positive definite matrix, which can be decomposed into $\mathbf{C}_N = \mathbf{D}\mathbf{D}^{tr}$ by means of a singular value decomposition. If the noise statistics are known, i.e. if the number of epochs is sufficiently high in order to obtain a good estimate of the noise covariance matrix, the process of data *pre-whitening* [Knösche *et al.*, to appear] can be used. Thus, we can restrict the theory to spatially uncorrelated noise where $\mathbf{D}$ is a diagonal weighting matrix. If we consider only one time point and Gaussian distributed and heteroscedastic (different in each channel) noise with zero mean, every channel i should be weighted according to its own noise standard deviation $\epsilon_i = |\underline{\Delta\Phi}_i^m|$ using the diagonal weighting matrix $\mathbf{D}^{-1}$ with entries $1/\epsilon_i$. This leads to the following algorithm for the instantaneous state TSVD ($n = 1$, α_i is a scalar):

- Calculate the singular system $\{\varsigma_i, \underline{u}_i, \underline{v}_i\}$ of the lead field matrix $\mathbf{L_q}$ by means of a singular value decomposition
- Choose $R > 1$, initialize $\underline{J} = 0$ and $i = 0$ and calculate $\bar{d} = ||\mathbf{D}^{-1}\underline{\Phi}_\epsilon^m||_2^2$
- While $\bar{d} > nR^2$:
  - Increase i by 1, calculate $\alpha_i = \underline{u}_i^{tr}\mathbf{D}^{-1}\underline{\Phi}_\epsilon^m$, $\underline{J} = \underline{J} + \frac{1}{\varsigma_i}\underline{v}_i\alpha_i$ and $\bar{d} = \bar{d} - \alpha_i^{tr}\alpha_i$
- $d = \bar{d}$, stop the procedure

T_γ is an order optimal regularization procedure ([Louis, 1989],[Vainikko, 1982],[Wolters *et al.*, 1997]). The greater the free parameter R is chosen, the stronger the regularization will be. Most of the following simulations in the sulcus structure have been

carried out with $R = 2$, but some results show that the choice $R \in [1.1, .., 1.5]$ would be more appropriate because of the small number r of source components.
The extension of the SA-TSVD to spatio-temporal modeling ($n > 1$) is straightforward for the moving and for the rotating dipole model. In these cases, $\underline{\alpha}_i$ is the $1 \times n$ vector

$$\underline{\alpha}_i = \underline{u}_i^{tr} \mathbf{D}^{-1} \mathbf{\Phi}_\epsilon^m,$$

$\frac{1}{\varsigma_i} \underline{v}_i \underline{\alpha}_i$ is an $r \times n$ matrix and the euclidian norm should be exchanged for the Frobenius-norm. The SA-TSVD can also simply be applied to the approximate approach of the fixed dipole model, described by [Mosher *et al.*, 1992]. In this approach, the dipole strengths for each dipole location tupel q are initially calculated under the assumption of rotating orientations. After that, the orientations are fixed by singular value decompositions of the $3 \times n$ submatrices $\mathbf{J}_i$ in $\mathbf{J} = (\mathbf{J}_1, \ldots, \mathbf{J}_p)^{tr}$, which describe the strengths in the three unit directions of every dipole. The fixed orientations are defined as the first left singular vectors of the submatrices $\mathbf{J}_i$. The appeal for this approximate approach lies in the reduced computational effort. A computationally more intensive implementation for the fixed dipole model could be the embedding of a projected gradient method or a penalty method for the determination of the two nonlinear orientation parameters into the SA-optimization process for the dipole locations and the calculation of the linear dipole strength parameters by means of the TSVD.

Methods

In the following study, the focal inverse current reconstruction methods without (SA-COF) and with regularization (SA-TSVD) are applied to a simulated sulcus structure in order to study their stability when overestimating the number of active sources and the spatial resolution of their reconstruction results in the sulcus.

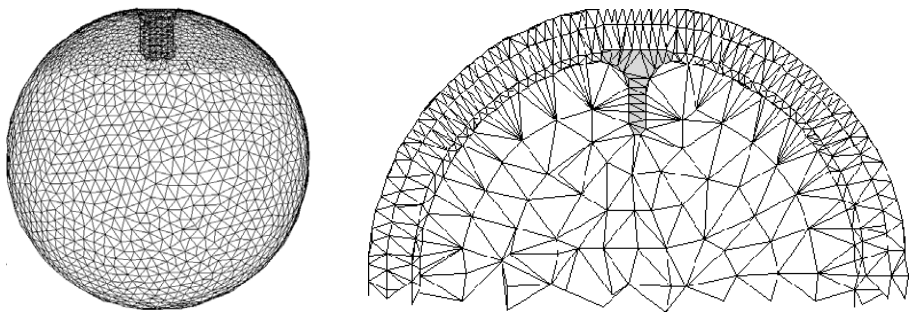

Figure 1: Tetraedra mesh of the four layer sphere model with embedded sulcus structure.

A four layer sphere model ($r_1 = 78mm$, $r_2 = 81mm$, $r_3 = 90mm$ and $r_4 = 96mm$) with a simulated sulcus embedded in the innermost sphere was constructed [Beckmann *et al.*, 1997]. Deeper in the sulcus the walls are parallel with a distance of $6mm$, the opening is described by two opposite hyperbolic functions. The sulcus has a depth of $22mm$ and a width of $17mm$. This model was read into the

CURRY [1] software-package in order to generate a 3D-tetraedral finite element mesh in CAUCHY-readable format respecting the segmented four surfaces of the model (figure 1). This led to 97581 tetraedra and 18213 nodes. The conductivities of the simulated skin and brain layers were set to $0.336(S/m)$, liquor conductivity to $1.0(S/m)$ and skull conductivity was set to $0.0042(S/m)$. 125 electrodes (1 reference electrode) were distributed regularly over the upper half of the skin surface (in accordance to the 10/10-system). The brain surface mesh was chosen as discrete influence space with 3446 influence nodes and the corresponding lead field matrix was calculated using the anatomical normal-constraint. The calculations were carried out in CAUCHY and visualization of reference sources and inverse results on the brain surface was done in CURRY.

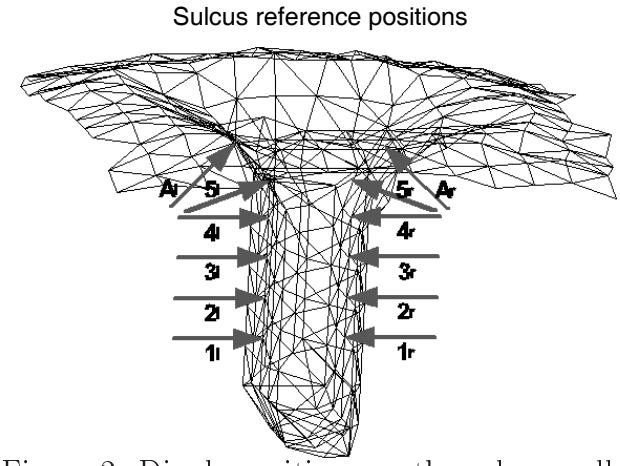

Figure 2: Dipole positions on the sulcus walls.

In the following simulations, reference sources were placed on surface mesh nodes of the sulcus (figure 2) and of the inner sphere and the potential distribution at the electrode locations was calculated using the lead field matrix. As a measure for the calculated field strength, we used the euclidean norm of the electrode potentials

$$||\underline{\Phi}^c||_2 = \sqrt{\sum_{i=1}^{124} (\underline{\Phi}^c)_i^2}.$$

Noise was then added and the resulting potential distribution was used to simulate the measurement data for the focal inverse source reconstruction. The noise was assumed to be Gaussian distributed with zero mean and heteroscedastic, thus D being a diagonal weighting matrix. The signal to noise ratio (SNR) was varied for the different simulations. It is defined as

$$SNR = \frac{\sum_{i=1}^{124} |\,(\underline{\Phi}_\epsilon^m)_i\,|}{\sum_{i=1}^{124} \epsilon_i}.$$

The focal inverse current reconstruction was then carried out using SA-COF and SA-TSVD with a varying number of dipoles. At first, the activity was limited to

[1] Philips research laboratories, Hamburg, Germany

one sulcus wall, then both sulcus walls were active and in the last simulation we used separated reference sources.

Results

Each of the deeper sources $1l$, $1r$, $2l$, $2r$, $3l$, $3r$ and $4l$, $4r$ with normalized strength $(100nAm)$ generated a calculated potential distribution of about $||\underline{\Phi}^c||_2 = 25\mu V$. Surface-near dipoles have a much greater effect on the electrode potentials, $5l$ and $5r$ of about $||\underline{\Phi}^c||_2 = 83\mu V$ and Al and Ar of about $||\underline{\Phi}^c||_2 = 71\mu V$.

Activity on one sulcus wall

Simulation 1

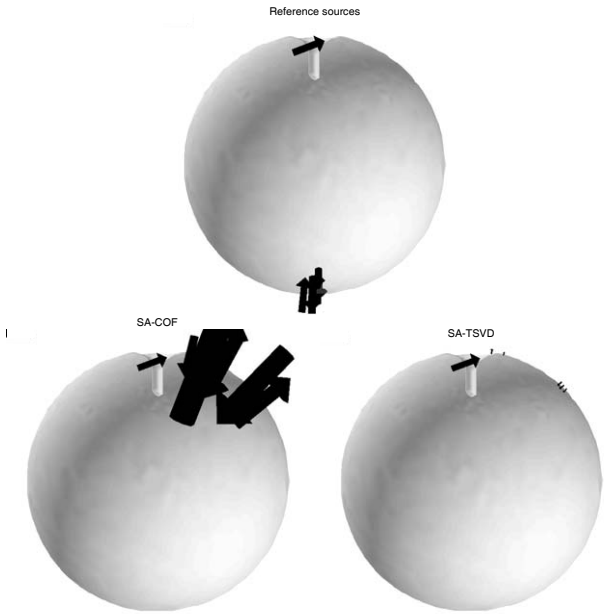

Figure 3: Reference dipole configuration (top) and the reconstruction results of the SA-COF (left) and SA-TSVD (right) when searching for 6 dipoles.

Six reference dipoles $(100nAm)$ were placed in the model (figure 3), one at the sulcus position $5l$ and five at the bottom of the inner sphere only to simulate biological noise (strength of the noise dipole potentials $||\underline{\Phi}^c||_2 \approx 4\mu V$).
In CAUCHY, forward results are stored with a precision of five digits. When carrying out a focal inverse source reconstruction SA-COF for six dipoles, using the stored potential values, the noise dipoles already could not be reconstructed in contrast to the sulcus source. Five dipoles on the bottom of the inner sphere were found with locations, differing slightly from the locations of the reference noise sources.
Noise with $SNR = 17.9$ was then added to the reference potentials with $||\underline{\Delta\Phi}^c||_2 = 19\mu V$. The goal of the inverse search cannot be the reconstruction of the noise

dipoles. It should be rather ensured that the left sulcus activity, lying above the noise level, can be emphasized in the result. Therefore, a single dipole model is appropriate and both algorithms, SA-COF and SA-TSVD yielded the right location $5l$ with an appropriate strength. In practice, the number of active sources is unknown. If for example two dipoles are underlying the measured potentials, the search for one source would not be a good model. In contrast to that, if the number of active sources is overestimated, a desirable result would be the reconstruction of the real sources and the neglect of the remaining ones by assigning small values of strength to them.
SA-COF and SA-TSVD were then carried out with six dipoles. The result is shown in figure 3. The defect d of the calculated potentials to the noisy data without regularization is $11\,(\mu V)^2$, with regularization it is $16.4\,(\mu V)^2$. Thus, despite being a better approximation to the measured data, the SA-COF is not stable. The activity in the sulcus was reconstructed (dipole $5l$ with a strength of $91nAm$), but stays behind a stronger activity of the remaining and only noise-explaining dipoles (strongest dipole $374nAm$). The regularization method focusses on the sulcus activity and avoids that the remaining defect to the data is explained by strong dipoles, which cancel each other with regard to their potential distribution or sources which have a small influence on the potential distribution, like deep sources (EEG and MEG) or radial sources (MEG). Fixing the dipole locations of the SA-COF result and considering the regularized solution of the resulting least square problem, the defect is about $19.6\,(\mu V)^2$. The first eigenvector $\underline{v}_1$ emphasizes the sulcus node $5l$ and already after the first term of the generalized inverse, the defect drops off below the noise level and the discrepancy principle takes effect.

Simulation 2

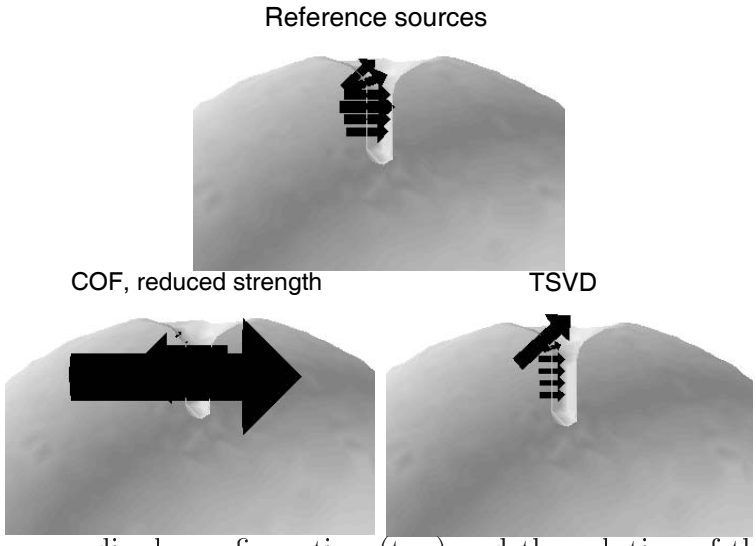

Figure 4: Reference dipole configuration (top) and the solution of the least square problem with the COF (left, ten times reduced dipole strength), and the TSVD (right), using the reference dipole locations.

Six dipoles were placed on the left sulcus wall at the positions $1l$ $(100nAm)$, $2l$ $(110nAm)$, $3l$ $(130nAm)$, $4l$ $(110nAm)$, $5l$ $(100nAm)$ and Al $(100nAm)$ (figure 4). Altogether, this led to a reference potential distribution of $||\underline{\Phi}^c||_2 = 195\mu V$. Low noise with a $SNR = 75.3$ $(||\underline{\Delta\Phi}^c||_2 = 30\mu V)$ was then added to these potentials. When fixing the reference dipole locations, figure 4 shows the solutions of the corresponding least square problem with the COF (ten times reduced dipole strength) and with the TSVD. The condition number of the corresponding lead field matrix $\mathbf{L_q}$ is 1960. Thus the least square problem is ill-conditioned and without regularization, the high frequency components of the noise are extremely amplified in the solution. Because the current density is assumed to be smooth for neighboring sources, the regularization is a justified and necessary model for noisy data. During the simulated annealing process, high condition numbers often appear for separated dipole locations. In this case, the model of regularization cannot be justified by the smoothness property of the current density and high frequencies in the source space can be quite meaningful. Here, the regularization can be seen as a method to ameliorate the condition of the problem. The high frequency components in the data space are lying below the noise level and thus, high frequencies in the source space cannot be reconstructed.

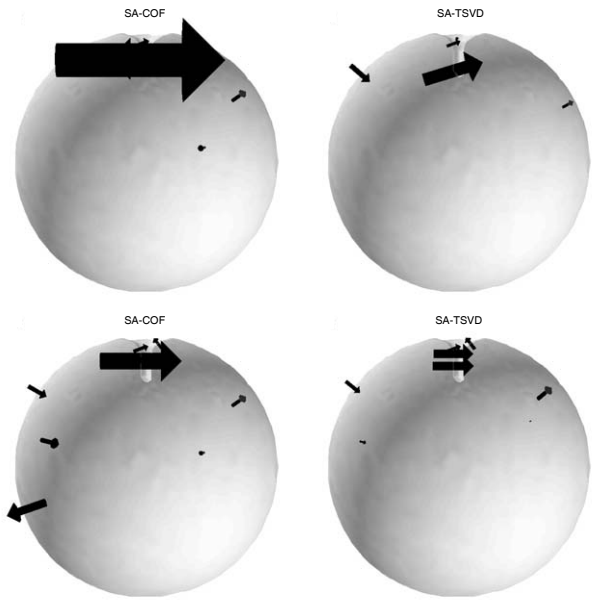

Figure 5: Reconstruction results of SA-COF (left) and SA-TSVD (right) when searching for 5 dipoles (top) and 8 dipoles (bottom).

SA-COF and SA-TSVD were carried out with five dipoles (figure 5). The result of the SA-COF has a defect of only $d = 25.8\,(\mu V)^2$, but is not stable with regard to the sulcus wall. The data is explained by a strong dipole on the left wall $(990nAm)$, weakened by a source on the right wall with opposite direction $(490nAm)$. The problem is ill-posed and the high frequency component had a strong influence in the result. The solution of the regularization method has a defect of $27.9\,(\mu V)^2$ and is stable concerning the sulcus wall but it should be mentioned that a result with

dipoles on both sulcus walls with the same direction can not be precluded.
In the following, eight dipoles were searched for (figure 5). Both algorithms show the main activity on the left sulcus wall. The spatial resolution of the SA-TSVD is better. It seems that the noise-flawed potential distribution of dipole Al can be explained by three dipoles, one at sulcus position Ar, a second on the left side of the sphere surface and a third at the same height on the right side of the sphere surface. With the SA-COF, a second part of the noise is explained by a deep and strong source, lying at the bottom left of the sphere surface, the method is getting unstable.

Activity on both sulcus walls

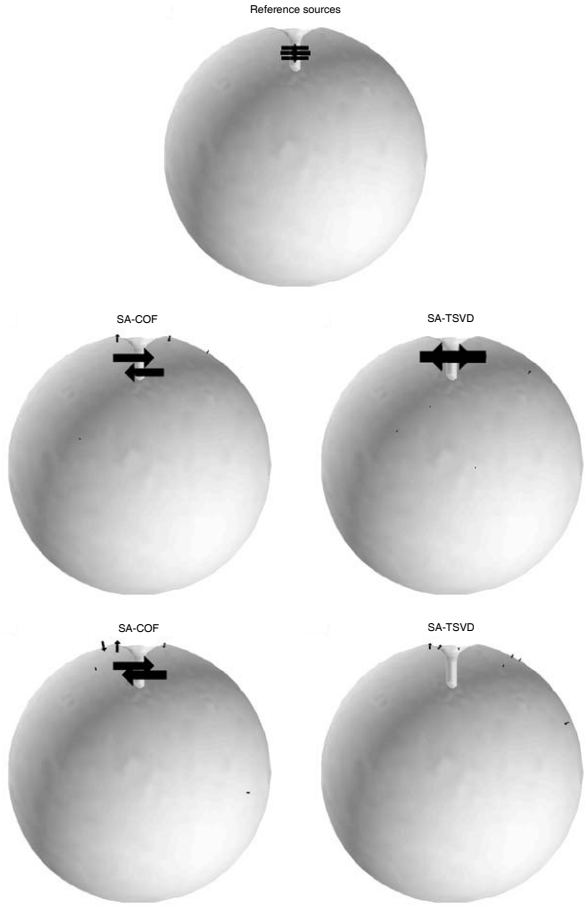

Figure 6: Reference dipole configuration (top) and reconstruction results of SA-COF (left) and SA-TSVD (right) when searching for 6 dipoles (middle) and 7 dipoles (bottom).

Six opposing dipoles were placed on the left and right sulcus wall at the positions $1l$ $(100nAm)$, $2l$ $(110nAm)$, $3l$ $(100nAm)$, $1r$ $(100nAm)$, $2r$ $(120nAm)$ and $3r$ $(100nAm)$ (figure 6). Because of the eliminating effect the total potential had an euclidian norm of only $||\underline{\Phi}^c||_2 = 36.8\mu V$. Noise yielding a SNR of 11.35 was added

to these potentials and the inverse reconstruction for 6 and 7 dipoles was carried out with both algorithms (figure 6). When searching for 7 dipoles, the SA-COF could reconstruct the sulcus activity with a defect of $d = 4.7\,(\mu V)^2$, while the SA-TSVD tended to a "zero-solution" and a defect of $d = 5.3\,(\mu V)^2$ was left to the data. The regularization with $R = 2.0$ was too careful with regard to the noise and to the high spatial frequencies of the source configuration.

Separated activity

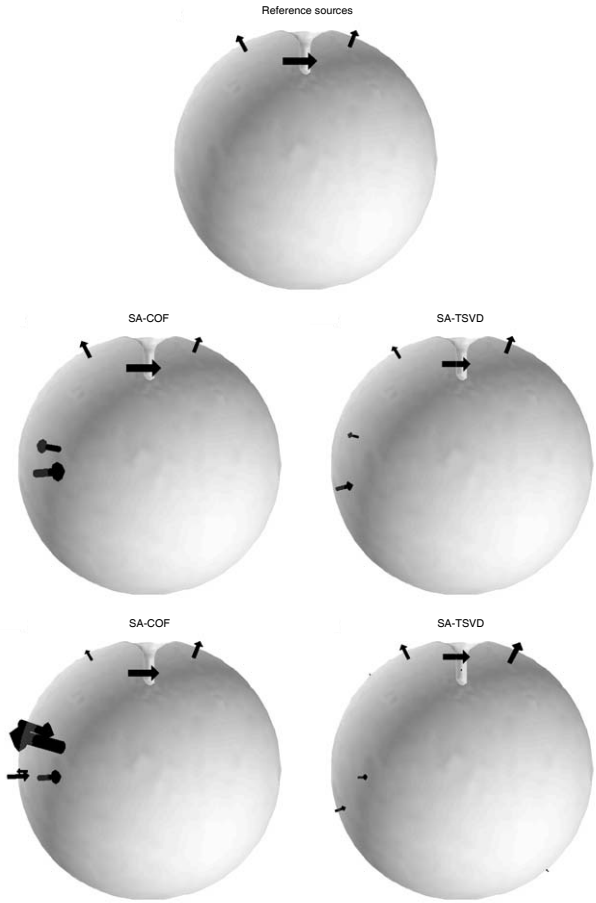

Figure 7: Reference dipole configuration (top) and reconstruction results of SA-COF (left) and SA-TSVD (right) when searching for 5 dipoles (middle) and 8 dipoles (bottom).

More than one active source region normally contributes to integrative processes of the brain and the locations of the involved sources can be quite separated. In the last simulation, three dipoles were placed in the sulcus structure, one on the left sulcus wall at position $1l$ ($200nAm$) and two further sources on the surface of the inner sphere ($100nAm$) (figure 7). The reference potential had an euclidian norm of $||\underline{\Phi}^c||_2 = 71\mu V$. Using these noiseless data, the SA-COF could exactly reconstruct the reference source configuration when searching for three dipoles.

Noise with $SNR = 16.6$ and $||\Delta\underline{\Phi}^c||_2 = 18.5\mu V$ was added to these potentials. When searching for three dipoles, the SA-COF, just like the SA-TSVD with the regularization parameter $R \in [1.1, \ldots, 1.5]$ could reconstruct the reference configuration with only a small localization error. The error for the SA-TSVD was more significant when choosing $R = 2.0$. In this case, the regularization is too careful and the loss of information is too large for the small dimension of the source space.
The inverse reconstruction for 5 and 8 dipoles indicates the stabilizing effect of the regularization (figure 7).

Discussion and Conclusions

We have presented a new regularization approach for nonlinear dipole fit algorithms and we have carried out simulations using the instantaneous state dipole model (single time slice of data, typically at the peak of the observed EEG/MEG-response). The focal inverse source reconstruction algorithm simulated annealing in combination with the regularization method TSVD shows good properties to determine "sure" sources. Dipoles which have a measurable effect on the data, will be reconstructed and do not sink into insignificance beside stronger and physiologically unexplainable sources which only explain noise and nearly cancel each other (EEG and MEG) or deep sources (EEG and MEG) or radial sources (MEG). The algorithm accounts for noise in the data, especially in combination with bad condition numbers of the least square problems, occuring during the inverse search. It especially seems to be more stable regarding an overestimation of the number of active dipoles when compared with conventional nonlinear dipole fit algorithms like it is the SA-COF. In combination with the singular value decomposition of the spatio-temporal data, giving an estimate for the minimal number, the exact number of dipoles can better be enclosed. This can be seen as a "trial and error" strategy of determining the number of sources, compared with the statistical concept of the information criteria, working in the data space [Knösche *et al.*, to appear] or the method based on the SVD of the measurement data, proposed by [Mosher *et al.*, 1992]. The strength of the regularization, controlled by the parameter R, should not be chosen too large, because it is proportional to the loss of information and because the dimension of the source space is small. The choice $R \in [1.1, \ldots, 1.5]$ for the TSVD showed the best performance during our simulations.
With regard to spatio-temporal modeling, as we have shown, the SA-TSVD can simply be extended to the moving dipole model (unconstrained location and orientation), to the rotating dipole model (fixed location, unconstrained orientation) and to the fixed dipole model approach, proposed by [Mosher *et al.*, 1992]. When embedding a further nonlinear algorithm to determine the two fixed orientation parameters during the SA-process for the location parameters, e.g. projected gradient methods or penalty methods, the concept of the SA-TSVD can also be applied to the fixed dipole model (fixed locations and fixed orientations). Nevertheless, it should be mentioned that this procedure will be quite computationally time-consuming.
The presented regularization concept can be of special importance, if dipole locations are already known (a-priori information, e.g. functional magnetic resonance imaging constrained dipole fits) whose corresponding lead field matrix is ill-posed.

In our sulcus simulations with the focal source model, the influence space was discretized with 3446 influence nodes. The normal-constraint had been applied, so that for every influence node only the strength parameter had to be determined. If reference activity is restricted to one sulcus wall and noise complicates the reconstruction, high spatial frequency inverse source configurations like dipoles on both sulcus walls having opposite directions can have a strong influence in the result of conventional dipole fit methods like the SA-COF. The SA-TSVD is more stable with regard to the sulcus wall, but it cannot be precluded that small dipoles on the opposite sulcus wall with the same dipole moment direction are added to explain the data. This is the principle of the shadow [Wang, 1994], who examined the MNLS-inverse (minimum norm least squares, distributed source model) in a simulated sulcus structure.
If both sulcus walls are active and the dipoles nearly cancel each other with regard to their surface potential distribution, the regularization method tends to the "zero-solution" proportional to the size of the regularization parameter R, to the noise in the data and to the chosen number of dipoles. The loss of information with a regularization of $R = 2.0$ and the choice of seven active dipoles during simulation was too strong to reveal the underlying sulcus activity. A choice of $R \in [1.1, \ldots, 1.5]$ or fewer dipoles was more adequate and even in the case of noisy data, the activity on both sulcus walls was reconstructed.

References

[Beckmann *et al.*, 1997] R. Beckmann, H. Buchner, and G. Knoll. Inverse localization of neuronal activity on opposite walls of a simulated sulcus. In *[Witte* et al., *1997]*, pages 484–486, 1997.

[Bertrand *et al.*, 1991] O. Bertrand, M. Thévenet, and F. Perrin. 3d finite element method in brain electrical activity studies. In *[Nenonen* et al., *1991]*, pages 154–171, 1991.

[Bio, 1996] Biomag96. *Proc. of the 10th Int.Conf.of Biomagnetism; Santa Fe*, 1996.

[Buchner *et al.*, 1997] H. Buchner, G. Knoll, M. Fuchs, A. Rienäcker, R. Beckmann, M. Wagner, J. Silny, and J. Pesch. Inverse localization of electric dipole current sources in finite element models of the human head. *Electroencephalogr. and Clin. Neurophysiol.*, 102:267–278, 1997.

[Fuchs *et al.*, 1998] M. Fuchs, M. Wagner, H.A. Wischmann, T. Köhler, A. Theißen, R. Drenckhahn, and H. Buchner. Improving source reconstructions by combining bioelectric and biomagnetic data. *Electroencephalogr. and Clin. Neurophysiol.*, 107:93–111, 1998.

[Fulton, 1938] J.F. Fulton. *Physiology of the Nervous System.* Ch.15. University Press, Oxford, London, 1938.

[Gerson *et al.*, 1994] J. Gerson, V.A. Cardenas, and G. Fein. Equivalent dipole parameter estimation using simulated annealing. *Electroencephalogr. and Clin. Neurophysiol.*, 92:161–168, 1994.

[Hämäläinen and Ilmoniemi, 1994] M.S. Hämäläinen and R.J. Ilmoniemi. Interpreting magnetic fields of the brain: minimum norm estimates. *Med. & Biol. Eng. & Comput.*, 32:35–42, 1994.

[Hämmerlin and Hoffmann, 1991] G. Hämmerlin and K.-H. Hoffmann. *Numerische Mathematik*. Springer-Verlag, 2 edition, 1991.

[Haneishi *et al.*, 1994] H. Haneishi, N. Ohyama, K. Sekihara, and T. Honda. Multiple current dipole estimation using simulated annealing. *IEEE Transactions on Biomedical Engineering*, 41:1004–1009, 1994.

[Haueisen *et al.*, 1995] J. Haueisen, C. Ramon, P. Czapski, and M. Eiselt. On the influence of volume currents and extended sources on neuromagnetic fields: A simulation study. *Annals of Biomedical Engineering*, 23:728–739, 1995.

[Knösche *et al.*, to appear] T.R. Knösche, E.M. Berends, H.R.A. Jagers, and M.J. Peters. Determining the number of independent sources of the EEG. a simulation study on information criteria. *Brain Topography*, to appear.

[Lorente de No, 1938] R. Lorente de No. Cerebral cortex: architecture, intracortical connections, motor projections. In *[Fulton, 1938]*, 1938.

[Louis, 1989] A.K. Louis. *Inverse und schlecht gestellte Probleme*. Teubner-Verlag, 1989.

[Marin *et al.*, 1998] G. Marin, C. Guerin, S. Baillet, L. Garnero, and Meunier G. Influence of skull anisotropy for the forward and inverse problem in EEG: simulation studies using the FEM on realistic head models. *Human Brain Mapping*, 6:250–269, 1998.

[Menon *et al.*, 1997] V. Menon, J.M. Ford, K.O. Lim, G.H. Glover, and A. Pfefferbaum. Combined event-related fMRI and EEG evidence for temporal-parietal cortex activation during target detection. *Neuro Report*, 8:3029–3037, 1997.

[Miller, 1979] K. Miller. Least squares methods for ill-posed problems with a prescribed bound. *SIAM Journal of Math. Analysis*, 1:52–74, 1979.

[Mosher *et al.*, 1992] J.C. Mosher, P.S. Lewis, and R.M. Leahy. Multiple dipole modeling and localization from spatio-temporal MEG data. *IEEE Transactions on Biomedical Engineering*, 39(6):541–557, 1992.

[Nenonen *et al.*, 1991] J. Nenonen, H.M. Rajala, and T. Katila, editors. *Biomagnetic localization and 3D Modelling*. Report Department of Technical Physics, Helsinki University, 1991.

[Nunez, 1990] P.L. Nunez. Localization of brain activity with electroencephalography. In *[Sato, 1990]*, pages 39–65, 1990.

[Opitz *et al.*, to appear] B. Opitz, A. Mecklinger, D.Y. von Cramon, and F. Kruggel. Combining electrophysiological and hemodynamic measures of the auditory oddball. *Psychophysiology*, to appear.

[Plonsey and Heppner, 1967] R. Plonsey and D. Heppner. Considerations on quasi-stationarity in electro-physiological systems. *Bull.math.Biophys.*, 29:657–664, 1967.

[Pohlmeier *et al.*, 1997] R. Pohlmeier, H. Buchner, and G. Knoll. The influence of skull-conductivity misspecification on inverse source localization in realistically shaped finite element head models. *Brain Topography*, 9(3):157–162, 1997.

[Rienäcker *et al.*, 1997] A. Rienäcker, H. Buchner, and G. Knoll. Comparison of regularized inverse EEG analyses in finite element models of the individual anatomy. In *[Witte* et al.*, 1997]*, pages 459–463, 1997.

[Sato, 1990] S. Sato, editor. *Magnetoencephalography.* Raven Press, New York, 1990.

[Scherg and von Cramon, 1985] M. Scherg and D. von Cramon. Two bilateral sources of the late AEP as identified by a spatio-temporal dipole model. *Electroencephalogr. and Clin. Neurophysiol.*, 62:32–44, 1985.

[Thompson and Patterson, 1974] R.F. Thompson and M.M. Patterson, editors. *Bioelectric Recording Techniques.* Part B. Academic Press, New York, 1974.

[Vainikko, 1982] G.M. Vainikko. The discrepancy principle for a class of regularization methods. *USSR Computational Mathematics and Mathematical Physics*, 22(3):1–19, 1982.

[Vainikko, 1983] G.M. Vainikko. The critical level of discrepancy in regularization methods. *USSR Computational Mathematics and Mathematical Physics*, 23(6):1–9, 1983.

[van den Broek *et al.*, 1996] S.P. van den Broek, H. Zhou, and M.J. Peters. Computation of neuromagnetic fields using finite element method and biot savart law. *Med. & Biol. Eng. & Comput.*, 34:21–26, 1996.

[Vaughan, 1974] H.G. Vaughan, Jr. The analysis of scalp-recorded brain potentials. In *[Thompson and Patterson, 1974]*, pages 158–207, 1974.

[Wagner *et al.*, 1994] M. Wagner, M. Fuchs, H.-A. Wischmann, R. Drenckhahn, and Th. Köhler. Current density reconstructions using the L1-norm. In *[Bio, 1996]*, pages 158–207, 1994.

[Wang, 1994] J.-Z. Wang. MNLS inverse discriminates between neuronal activity on opposite walls of a simulated sulcus of the brain. *IEEE Transactions on Biomedical Engineering*, 41(5), 1994.

[Witte *et al.*, 1997] H. Witte, U. Zwiener, B. Schack, and A. Doering, editors. *Quantitative and Topological EEG and MEG Analysis.* Druckhaus Mayer Verlag GmbH Jena · Erlangen, 1997.

[Wolters *et al.*, 1997] C. Wolters, A. Rienäcker, R. Beckmann, H. Jarausch, H. Buchner, R. Grebe, and A.K. Louis. Stable inverse current reconstruction in real anatomy using combinatorial optimization techniques combined with regularization methods. In *[Witte* et al.*, 1997]*, pages 487–490, 1997.

[Wolters, 1997] C. Wolters. Direkte Methoden zur Berechnung dipolinduzierter elektrischer und magnetischer Felder und inverse Strategien zur Quellokalisation im Gehirn. Diplomarbeit in Mathematik mit Nebenfach Medizin, Institut für Geometrie und Praktische Mathematik, RWTH Aachen, 1997.

[Wood, 1982] C.C. Wood. Application of dipole localization methods to source identification of human evoked potentials. *Ann. New York Acad.Sci.*, 388:139–155, 1982.